IASMiRT

SMiRT 26
50 Anniversary Berlin/Potsdam

Transactions, **SMiRT-26**
Berlin/Potsdam, Germany, July 10-15, 2022
Division I

Creep Response in Ultra-High-Performance Concrete

Ryan Rogowski[1], Christopher Jones[1], Robert Peterman[1]

[1] Kansas State University, Manhattan, KS, USA

ABSTRACT

With increased usage among today's modern infrastructure, ultra-high-performance concrete (UHPC) and its mechanical properties have been the focus of many research projects and experiments. Understanding the advantages of this relatively new material can provide immense benefits in design of global infrastructure. The purpose of this study is to fill the gaps in understanding of long-term deformation behavior and structural significance of UHPC mixtures by accurately measuring and modelling the creep strain observed in UHPC specimens. A series of six, 2.5" by 2.5" by 36" column specimens were tested, three cast with normal strength concrete and three cast with ultra-high-performance concrete. The specimens were loaded to varying stress levels defined as fractions of measured f'c values for a duration of 28 days. Displacement measurements were taken at predetermined time intervals using a Whittemore gauge and embedded brass inserts. The data collected for each specimen was fitted using a Laplace transform elastic-viscoelastic solution. The fitted data was the used to show and compare calculated values of creep compliance and creep coefficients for the various stress levels of each concrete mix. The creep compliance values after 28 days for the normal strength concrete ranged from 3.09E-07 to 3.75E-07 psi^{-1} and the 28-day creep coefficients ranged from 1.33 to 2.51. The creep compliance values after 28 days for the ultra-high-performance concrete ranged from 2.31E-07 to 2.35E-07 psi^{-1} and the 28-day creep coefficients ranged from 1.39 to 1.48. The modeled creep curves and their respective fit parameters are presented in addition to the calculated values of creep compliance and creep coefficients.

INTRODUCTION

Since its inception in the 1980's ultra-high-performance concrete (UHPC) has been a popular topic among the infrastructure industry (Schmidt and Fehling, 2004). The materials superior properties have drawn engineers to its potential usage in modern construction. When compared to normal strength structural concrete, UHPC mixtures have shown greater strength and durability properties. Mainly characterized by high tensile strengths ranging from 1.2 to 2.2 ksi (Wille et al, 2011) and compressive strengths ranging from 17 to 22 ksi (Tadros et al., 2020) engineers quickly realized the advantages to using UHPC mixes in both traditional and "tensioned" concrete design. Though it has been used primarily for bridge applications, UHPC has begun to make an impact in the nuclear infrastructure community as well. Using UHPC mixtures for reactor safety structures could provide increased safety benefits due to its low porosity as well as reductions in material and construction cost.

UHPC mixtures gain their increased strength and durability behavior by applying four principle adjustments to the mix matrix of normal strength concrete (NSC). These include a reduction in the water-cement-ratio (w/c) to 0.25 or less, elimination of coarse aggregate to achieve greater packing density, the use of additional superplasticizers to maintain workability and the incorporation of fibrous materials to increase the tensile properties (Schmidt and Fehling, 2004).

While plenty of research has been done on ultra-high-performance concrete in the past thirty years there is still a need for more information to help validate and create safe code provision for designers in the years to come. Among the available research, projects have included studying better material substitutes for cheaper and stronger mixtures, finding different curing methods for increase strength, or observing the effectiveness as structural members such as beams or columns. However, while in most of these projects the materials strength properties are normally well recorded there is a lack in information about the time-dependent properties such as the creep or shrinkage seen with UHPC mixtures. These time-dependent properties are vital to designers and if neglected during the design process, will lead to inadequate structures. For example, a major aspect of pretension or post-tension design is the importance of losses. Losses are a reduction in the tensioning forces applied to a member due to immediate and long-term deformations in both the concrete and steel strands (Nawy, 1996). A major factor of the losses due to long-term deformations are the creep strains that develop within the concrete member from the effect of the constant compressive force being applied. If not taken into consideration during, these losses will cause excess deflections which in turn create cracking and ultimately failure. Knowing the level of importance that these long-term deformation behaviors hold in design, it is necessary that for further advancements in structural design the creep properties of a UHPC material should be well known and documented.

The scope of this research is to fill in gaps in the understanding as well as reinforce previous research conclusions over the time depended deformation properties of normal strength concrete (f'c~6ksi) and ultra-high-performance concrete (f'c~21ksi). A series of three test specimens for each mix were loaded to selected stress levels and held at constant for a 28-day period in a temperature and humidity-controlled room. The concrete deformations were measure at selected time intervals via external Whittemore strain gauge readings between embedded brass inserts on the side of the test specimens. The collected data was used to accurately model the time dependent deformation properties of both concrete mixes by determining fit parameters for a Laplace Transform Elastic-Viscoelastic solution. The creep compliance and creep correlation values were calculated and compared to values found in previous research.

THEORY

Concrete is a viscoelastic material, meaning upon loading a linear stress-strain relation can be observed. However, after holding a load constant the material shows signs of viscous behavior with a reduction in the strain rate due to particle redistribution. This behavior, notable know as creep, is debated amongst material engineers today as many factors play into the creep behavior of a concrete mixture. Separating concrete into its two main components, the aggregates and cement paste, it has been agreed upon that creep is not a factor of the aggregates and instead the question of what causes creep is left to be discussed solely by the behavior of the cement paste. A common consensus is that creep occurs as a product of the rearrangement of the cement paste nanostructure due to the presence of water in Calcium-Silicate-Hydrate (Hailong Ye, 2015). Where, the interaction between the water and the calcium silicate hydrate cause deformations due to either movement of free water between pores, redistribution of particles through sliding or transfer caused by the absorbed water, or translation of internal molecular structure due to the interlayer water.

To determine creep properties of concrete it is common to load concrete test specimens to stress levels up to 50% of the measured f'c value. Doing this ensures that the concrete will remain in a linear elastic behavior. Keeping the applied stress below 0.50f'c allows for the simplification of calculations while still producing accurate data modeling using constitutive equations. These equations are modeled using different arrangements of springs and dashpots to replicate the elastic and viscous behaviors seen. In doing so, the springs will represent the elastic properties and the dashpots help to model the viscous behavior of concrete (Findley et al, 1976).

Two basic models for viscoelastic solutions are the Maxwell and Kelvin models. The Maxwell model consist of a spring and dashpot arranged in series. While adequate for determining the initial elastic strain behavior it falls short to accurately represent the creep strain behavior due to a lack of creep strain rate differentiation. The Kelvin model consists of a spring and dashpot arranged in parallel. Unlike the Maxwell model, the Kelvin model more accurately depicts the creep strain rate behavior seen in time dependent tests of concrete. However, the Kelvin model does not include an initial elastic strain component. Due to their differences the two models are commonly used together to form combined three or four element models that work together to capture the full-time dependent strain behavior observed in tests (Findley et al, 1976). Using the simple stress-strain relationship equations for both a spring and dashpot, total stress or total strain equations can be created and manipulated using LaPlace transforms to form a strain function with respect to time to fit recorded data.

Creep data is commonly presented in two ways, the first being the calculation of a creep compliance, which is a measurement of the creep strain per unit stress shown in equation 1. The second is the presentation of the calculated creep coefficient, equation 2, which shows the ratio of creep strain to initial strain (ACI 209, 2008).

$$J(t) = \frac{\varepsilon(t)_{cr}}{\sigma} \tag{1}$$

$$C = \frac{\varepsilon(t)_{cr}}{\varepsilon_0} \tag{2}$$

Similar to a strain function found with the three-element model mentioned above the viscoelastic solution presented in equation 3 was formed with fit Parmenter's E0, E1, τ, β and Pmax. To obtain this function the time variable was removed using Laplace transforms in a similar manor as done by Jones and Grasley in their research on short-term creep of cement paste during nanoindentation (Jones and Grasley, 2010).

$$\varepsilon(t) = \left(\frac{1}{E_0} + \frac{1 - e^{-\left(\frac{t}{\tau}\right)^{\beta}}}{\left(1 - \frac{1}{e}\right) E_1} \right) * \frac{P_{max}}{A} \tag{3}$$

Initially assuming the load is applied as a step load allows for the Laplace transform of the step function to be taken as seen in equation 4 and will be used when taking the inverse Laplace transform in later stages.

$$P(s) = \frac{P_{max}}{s} \tag{4}$$

The transformed relaxation modulus in equation 5 includes the transformed creep compliance function. This transformed creep compliance function was derived from the creep compliance function presented by Jones and Grasley in equation 6.

$$\hat{E}(s) = \frac{1}{s^2 \hat{J}(s)} \tag{5}$$

$$J(t) = \frac{1}{E_0} + \frac{1}{E_1(1 - e^{-1})}(1 - e^{-\left(\frac{t}{\tau}\right)^{\beta}}) \tag{6}$$

To form equation 3, the inverse Laplace transform of the transformed stress function divided by the transformed relaxation modulus, as shown in equation 7, was equated. In doing so the output function was a strain function with relation to time, influenced by creep compliance multiplied by the applied stress.

$$L^{-1}\{\frac{P(s)/A}{s\hat{E}(s)}\} \tag{7}$$

LITERATURE REVIEW

As the phenomenon of creep has been observed since the early 1900's the creep behavior in NSC has been well documented, inversely, creep data covering UPHC mixtures is relatively limited. However, while limited there are available resources that begin to shed light on the creep behaviors of UHPC. Test performed under sponsorship of the FHWA (Graybeal, 2006; Haber et al., 2018) have provided some insight into the creep behaviour of UHPC mixtures. Graybeal conducted test loaded to 0.40f'c with varying curing regimes where he then recorded the creep coefficients from the observed data. The recorded coefficients were 0.29, 0.78, 0.66, 0.31 for steam treated, untreated, tempered steam treated, and delayed steam treated respectively. Haber et.al. continued with Graybeal's work by observing the creep coefficients recorded from different commercial mixtures at load levels of 0.40f'c and 0.65f'c. His research showed coefficients to range from 0.70 to 1.17 and 0.78 to 2.47 for the 0.40f'c and 0.65f'c stress levels respectively. The data presented in this research will add to the known knowledge of creep coefficients presented by Graybeal and Haber et.al., as well as expand on their research by providing results on the values of creep compliance with time.

MATERIALS

Normal Strength Concrete Mix Design

Following traditional concrete design procedures, a normal strength concrete mix was created. The mix used in this experiment had a desired f'c of 6 ksi after 28 days of curing. The w/c ratio was kept to 0.45 and a water reducer was added to help obtain greater compressive strength. Type I Portland Cement was used to form the cement paste and oven dried crushed stone and oven dried river sand formed the aggregates. Table 1 shows the proportioning for the normal strength concrete mix used in testing.

Table 1: Normal strength concrete mix design

Material	Specific Gravity	per cubic yard
Type I Portland Cement	3.15	564 lbs
Fine Aggregate	2.6	2024 lbs
Coarse Aggregate	2.6	1120 lbs
Water	1.0	254 lbs
Water Reducer – ADVA 140 M		25 fl. oz.

Ultra-High-Performance Concrete Mix Design

Over the years there have been several UHPC mixtures that have been available for commercial usage. While each have their differences, ultra-high-performance concrete mixtures can be characterized by having a low water-to-cement ratio, high packing density, and include the usage of superplasticizers and steel fibers. For this experiment a mixture was derived from a UHPC mix design provided by HiPer Fiber LLC. This mix was formed through a study done to create an "open-recipe" UHPC mix that would be used as an alternative to expensive proprietary mixtures currently on the market (El-Tawil et al., 2020). Having a non-proprietary mix formula allowed for adjustments in the mix design to be made to better suit the needed requirements. The mix used in this test differed from the one described by HiPer Fibers, after numerous test batches it was decided to forego using silica fume and steel fibers as greater compressive strengths were seen without them. The desired f'c for the UHPC mixture was set at 21 ksi after 28 days of standard curing. The mix used had a w/c ratio of 0.18 and included a high range water reducer to maintain a high workability. Type I Portland Cement and Ground Granulated Blast Furnace Slag (GGBS) cement were used for the paste and a kiln dried fine sand produced by Quikrete was used as the fine aggregate. The addition of an accelerant helped to increase the 28 day compressive strength even further. Table 2 shows the used mix proportions for the UHPC test specimens.

Table 2: Ultra-high-performance concrete mix design

Material	Specific Gravity	per cubic yard
Type I Portland Cement	3.15	870 lbs
GGBS	2.81	870 lbs
Fine Aggregate	2.6	2100 lbs
Water	1.0	305 lbs
Water Reducer – Advocast 575		20 lbs
Accelerator – Daraset 400		348 fl. Oz.

Experimental Setup

Loading was applied using a screw driven mechanical jack creep frame apparatus. This setup allowed for the ability to apply a constant stress without loss of load. Fitted to the top of the frame was a 100-kip load cell which fed direct real time voltage readings to a Keithley 2750 multimeter/switch system where the voltage readings were converted into applied load readings in a custom lab-view based software.

The load frames used for testing had a large 36" space between jack and load cell. To fit this, a custom mold was designed for casting of test specimens. Due to the load limitation of the 100-kip load cells, a 2.5" by 2.5" cross section was used to allow for the proper load to be applied in relation to the desired stress. With such a small column member buckling failure was checked using Euler's equation for buckling, the 36" unbraced length and 2.5" by 2.5" cross section of the test specimen was determined to be adequate for pure compression without bending. Additionally, during the tests the measured strain differences between opposite sides would confirm relatively zero bending.

To measure the strain, a Whittemore gauge with a gauge length of 8" was used to manually measure length changes between embedded brass inserts. Experimental readings were recorded using a Mitutoyo ABS Digimatic indicator mounted to the Whittemore gauge which provided capabilities for an absolute zero setting and error of 0.0001 inches. The recorded readings were placed into a pre-set excel sheet via a Mitutoyo USB input tool to help eliminate recording errors. The brass inserts were set in line down the center of each side of the test specimen. These inserts were spaced at approximately 1" spacings and totaled to 34 inserts per side leaving a 1.5" space between a the top and bottom of the test specimen.

METHODS

Mix Procedure

Due to the limitation of having only two creep frames, two separate batches of normal strength concrete and two separate batches of ultra-high-performance concrete were mix on different days. Using the mix procedure provided by HiPer Fiber solutions for "Plant Mixing" the following steps were conducted to batch the UHPC mixtures after all ingredients were measured and proportioned for the desired batch size.

1. Silica Sand, Type I Cement and Slag were added to the mixer and dry-mixed for roughly 5 minutes
2. Water and HRWR were mixed separately before being added to the dry mixed materials
3. Accelerator added to the mix after the water and HRWR
4. Batch mix for approximately 30 minutes or until adequate mixture consistency was achieved

After mixing, the concrete was place into the 2.5” by 2.5” by 36” molds prepared with a 2.5” by 2.5” by ¼” steel cap placed at each end to help achieve a flat surface for load application. Temporary drilled steel spacers were set in channels within the molds to hold the brass inserts in place during the first 24 hours of curing. In addition to the test specimen molds, six 4” by 8” cylinders were also prepared to be used to check 7 and 28 day compressive strength of each mix. All molds were vibrated on a small vibrating table to allow for even dispersion of the concrete and reduction of air voids. The molds were then placed into a curing room at 95% RH and 23ºC and left for 24 hours before being demolded. All specimens were then placed back into the curing rooms to undergo standard moist curing for 28 days.

Loading Procedure

The 4” by 8” cylinders were pulled from the curing room at 7 and 28 days to check for compressive strength. At 28 days the test specimens were also pulled from curing at which point they were transferred to the creep frame in figure 1, where they then adjusted before taking on load. A total of six specimens

Figure 1: Test specimen loaded into creep frame

were tested under loading, three normal strength and three UHPC. Each specimen would be loaded to a percentage of the normal strength concrete or UHPC’s desired f’c values. The normal strength concrete test specimens were loaded to stress levels of 30,40 and 50% of the desired 6 ksi f’c value. This correlated to 35, 37, 58% respectively of the actual measured f’c values of each batch. The UHPC concrete test specimens were loaded to stress levels of 27,30 and 40% of the desired 21 ksi f’c value. This correlated to 32, 34 and 47% respectively of the actual measured f’c value of each batch. The loads applied to each specimen were held constant for the 28 day test and would be adjusted if seen to deviated more than 2% from the desired stress level. Two additional test specimens were kept unloaded and used to measure the free shrinkage of both NSC and UHPC mixtures.

Measurement Procedure

Measurements were performed using the Whittemore gauge previously mentioned by taking the deformation readings between the brass insert points along all the sides of each test specimen. Before taking a set of readings the Whittemore gauge was zeroed using a controlled gauge length of 7.965 inches. After zeroing, measurements were taken starting at the top of the column and then moving down towards the base. This process was repeated for each side measured. These readings were taken before and after initial loading, then at times of 3 hours, 6 hours, 9 hours, 24 hours, 48 hours, 72 hours, 1 week, 2 weeks, 3 weeks and 4 weeks after loading. The UHPC specimens had additional readings at times of 30 minutes, 1 hour and 12 hours after loading.

RESULTS AND DISCUSSION

As previously mentioned, compressive tests were performed on the 4" by 8" cylinders after 7 day and 28 day curing periods to determine the actual f'c value per mix batch. The recorded compressive strengths for both the NSC and UHPC can be seen below in tables 3 and 4 respectively.

Table 3: 7 day and 28 day compressive strengths for NSC mixes

Mix Batch	Normal Strength # 1	Normal Strength # 2
7 Day Compressive Strength (psi)	2,600 \ 3,560 \ 2,900 Avg. = 3,020	5,366 \ 5,807 \ 5,684 Avg. = 5,619
28 Day Compressive Strength (psi)	6,903 \ 4,128 \ 4,503 Avg. = 5,178	6,950 \ 6,790 \ 5,878 Avg. = 6,539

Table 4: 7 day and 28 day compressive strengths for UHPC mixes

Mix Batch	UHPC # 1	UHPC # 2
7 Day Compressive Strength (psi)	16,434 \ 15,871 \ 15,786 Avg. = 16,030	15,484 \ 15,496 \ 14,407 Avg. = 15,129
28 Day Compressive Strength (psi)	19,028 \ 18,234 \ 18,780 Avg. = 18,681	17,837 \ 17,797 \ 17,963 Avg. = 17,866

After the 28 day creep tests had concluded, the collected data was then post processed to be set up for data modelling. The procedure of post processing of the data was completed as follows. Beginning with the raw data readings the "zero" length of 7.965" was added to all recorded values to get the true distance between insert points. Next, using the traditional strain equation, the measured strain at each time interval was calculated. When determining the measured strain an "IF" statement was written into the strain equation to eliminate negative strain measurements as it can be assumed that under compressive load, increases in the specimen length are improbable. After the strain was calculated, the data was then averaged by taking the average of the individual insert point for all sides. With the average strains calculated, the data fitting was then performed. For the fitting procedure the average strains were separated by each insert point to be individually fit using equation 3 and a solver tool in excel. Before fitting, one further filtering occurred to eliminate additional outlier. These outliers included points that caused peaks or troughs in the viscoelastic curve that were evidently out of form. A similar procedure was performed to obtain the free shrinkage strain values where the strain fitting was done using the shrinkage equation provided by the ACI 209 specification as opposed to the equation 3 used prior.

Figure 4(a) shows the fit curve for an induvial insert point on the UHPC 0.40f'c test specimen. After determining the fit parameters E0, E1, τ, β and Pmax for each insert point they were averaged and used to form a best fit model like the one seen in figure 4(b) for the UPHC 0.40f'c test specimen. The calculated model strain values were then compared to the averaged strain values to determine the standard deviation and find the 95% confidence intervals for each test.

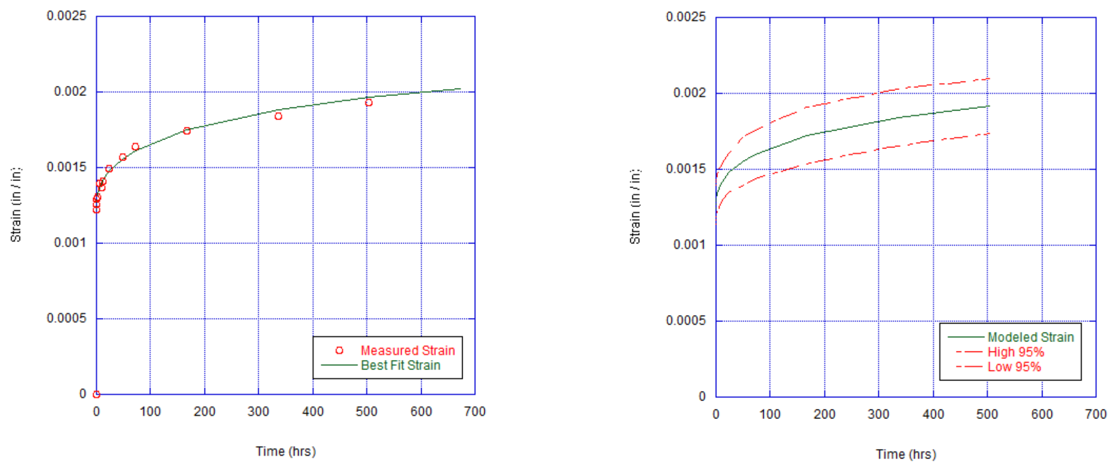

(a) (b)

Figure 4: (a) Data fit curve for individual mearusrement point on UHPC 0.40f'c test specimen (b) Curve for UHPC 0.40f'c test specimen with 95% confidence intervals

After determining the fit parameters for each test as seen in table 5, the creep compliance, J(t), was calculated using equation 4. The creep compliance data was normalized by subtracting the initial compliance, J(0), from the creep compliance, J(t). Shown below in figure 5(a) is the creep compliance curve over time for each of the six test specimens and in figure 5(b) the normalized creep compliance curves over time are presented.

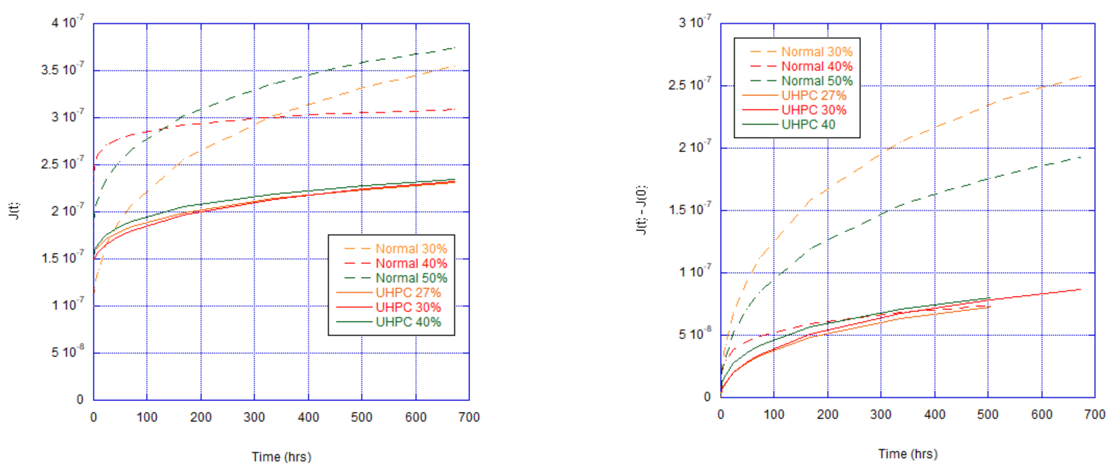

(a) (b)

Figure 5: (a) Creep compliance verse time curve (b) Normalized creep compliance verse time curve

Table 5: Strain vs time, Equation 1, fit parameters for individual test specimens

	E0	E1	β	τ	P
	(psi)	(psi)		(hrs)	(lbs)
Normal 30%	10338781.5	3885760.0	0.5100	672.0	11250.0
*Normal 40%	4303871.7	13672321.2	0.2981	504.0	15000.0
Normal 50%	5473752.6	5201520.0	0.5030	672.0	18750.0
*UHPC 27%	6616370.6	12561599.3	0.5289	672.0	35437.5
UHPC 30%	6855795.5	11549790.5	0.5573	672.0	39375.0
UHPC 40%	6738482.4	11580237.0	0.4500	672.0	52500.0

Table 6: initial and 28 day creep compliance and 28 day creep coefficients

	J(0)	J(t)28	C28
	(psi^-1)	(psi^-1)	
Normal 30%	9.67E-08	3.54E-07	2.51
*Normal 40%	2.32E-07	3.09E-07	1.33
Normal 50%	1.83E-07	3.75E-07	1.69
*UHPC 27%	1.51E-07	2.31E-07	1.39
UHPC 30%	1.46E-07	2.32E-07	1.46
UHPC 40%	1.48E-07	2.35E-07	1.48

Shown in table 6 are the initial and 28-day creep compliance values along with the 28-day creep coefficient values for each of the six tests performed. The two "asterisk" test, Normal 40% and UHPC 27%, are shown but should be considered defective. The test specimen for the Normal 40% test was allowed to dry before loading. While not intentional, the drying of the specimen before loading meant that free shrinkage would not be as great of an influence on this test as it would for other. As expected with this specimen a larger stiffness value, E1, was seen and lower creep compliance and creep coefficient values were recorded. The lower values can be attributed to the exclusion of free shrinkage strains. The test specimen for the UHPC 27% test was damaged upon loading, as a crack formed from the bottom of the specimen and propagated up. Original a desired stress level of 0.5f'c was set, but with the formation of the crack the test was to drop to a stress of 0.27f'c where no further cracking was observed and the load was held steady. Continuing to test this specimen highlighted the durability of UHPC mixtures as even when cracked the test specimen showed similar stiffness, creep compliance and creep coefficient values as those recorded in the uncracked UHPC 30% test.

As seen with the recorded values in tables 5 and 6, as well as the modeled curves shown in figure 5 it is evident that the UHPC test specimens are less susceptible to creep behavior when compared to NSC. While not conclusive it can be noted that through this experiment that the lower w/c ratio paired with a higher particle packing density of the UHPC mixture had an effect on the creep behavior seen. This was inferred as previously mentioned, creep is a product of the interaction of water and C-S-H. Reducing the w/c ratio with reduce the water content available to interact with the C-S-H thus showing a decrease in creep. Additionally, the high particle packing density eliminates the large spaces between aggregates which in turn reduces the amount of free water being trapped within the mixture which would lead to voids after drying.

Comparing the creep compliance values calculated in this experiment to those observed in previous research it is evident that there is an agreement with the long-term deformation behavior of

UHPC mixes. In their research, both Graybeal and Haber et.al. both performed tests on UHPC specimens to stress levels of 0.40f'c and obtained creep coefficient values ranging from 0.29 to 1.17. While these are lower than values calculated in this research, the 0.65f'c test performed by Haber showed a coefficient range from 0.78 to 2.47 which would encompass those values seen in table 6. The difference in coefficients for the 0.40f'c test can be attributed to the greater measured compressive strengths of the test specimens used both Graybeal and Haber et.al. in their research.

CONCLUSION

The data in this research confirmed the results presented in previous projects by Graybeal and Haber et.al. with the comparison of calculated creep coefficients for UHPC mixtures. It also provided new data in the form of a calculated creep compliance of UHPC mixtures which shows the long-term creep behaviour can be accurately modeling using elastic-viscoelastic solutions. The recorded data also shows that when compared to normal strength concrete, the UHPC mixtures are less susceptible to creep effects. The data presented in this experiment will help to create a full understanding of creep behavior of ultra-high-performance concrete mixtures as the values shown in this paper will add to ideas and results of past, current and future research projects.

ACKNOWLEDGEMENT

This research was supported by the U.S. Nuclear Regulatory Commission award number 31310021M0006. The opinions expressed in this study are those of the author(s) and do not reflect the views of the sponsors.

REFERENCES

Akhunoukh, A.K., Buckhalter, C., (2021). "Ultra-high-performance concrete: Constituents,mechanical properties, applications and current challenges," *Case Studies in Construction Materials*, Vol. 15.

American Concrete Institute 209, (2008). *Guide for Modeling and Calculating Shrinkage and Creep in Hardened Concrete*, Farmington Hills, MI.

El-Tawil, S., Tai,Y., Belcher, J. A., Rogers, D. (2020). "Open-Recipe Ultra-High-Performance Concrete," *Concrete International*, ACI, Vol. 42 No. 6, pages 33-35.

Findley, W.N., Lai, J.S., Onaran, K., (1976). *Creep and Relaxation of Nonlinear Viscoelastic Material With an Introduction to Linear Viscoelasticty*, Dover Publications, Mineola, NY, pages 50-77.

Graybeal, B., (2006). "Material Property Characterization of Ultra-High Performance Concrete," Federal Highway Administration, McLean, VA, pages 110-115.

Haber, Z.B., De la Varga, I., Graybeal, B.A., Nakashoji, B., El-Helou, R., (2018). "Properties and Behavior of UHPC-Class Materials," Federal Highway Administration, McLean, VA, pages 79-89.

Hailong, Y., (2015). "Creep Mechanisms of Calcium-Silicate-Hydrate: An Overview of Recent Advances and Challenges," *International Journal of Concrete Structures and Materials*, pages 453-462.

Jones, C.A., Grasley, Z.C., (2010). "Short-term creep of cement paste during nanoindentation," *Cement and Concrete Composites*, Vol. 33 No. 1, pages 12-18.

Nawy, E.G., (1996). *Prestressed Concrete A Fundamental Approach Second Edition*. Prentice-Hall, Upper Saddle River, NJ, page 72.

Schmidt, M., Fehling, E., (2004). "Ultra-High-Performance Concrete: Research, Development and Application in Europe," pages 3-5.

Tadros, M.K., Gee, D., Asaad, M., Lawler, J. (2020). "Ultra-High-performance concrete: A game changer in the precast concrete industry," *PCI journal*, PCI, Chicago, IL, Vol. 65. No.3, pages 33-25.

Wille, K., Naanam, A.E., El-Tawil, S., (2011). "Optimizing Ultra-High-Performance Fiber-Reinforced Concrete," *Concrete International*, ACI, Farmington Hills, MI, page 3.